Aggregation/Fibrillogenesis of Recombinant Human Prion Protein and Gerstmann−Sträussler−Scheinker Disease Peptides in the Presence of Metal Ions†

Fernanda Ricchelli,‡ Raffaella Buggio,‡ Denise Drago,‡ Mario Salmona,§ Gianluigi Forloni,§ Alessandro Negro,|| Giuseppe Tognon,‡ and Paolo Zatta*,‡

Department of Biology, CNR Institute of Biomedical Technologies/Metalloproteins Unit and Department of Biological Chemistry, University of Padova, Viale G. Colombo 3, 25121 Padova, Italy, and Institute of Pharmacological Research "Mario Negri", Via Eritrea 62, 20157 Milano, Italy

Received January 23, 2006; Revised Manuscript Received April 5, 2006

ABSTRACT: In this study we investigated the role of Cu^{2+}, Mn^{2+}, Zn^{2+}, and Al^{3+} in inducing defective conformational rearrangements of the recombinant human prion protein (hPrP), which trigger aggregation and fibrillogenesis. The research was extended to the fragment of hPrP spanning residues 82−146, which was identified as a major component of the amyloid deposits in the brain of patients affected by Gerstmann−Sträussler−Scheinker (GSS) disease. Variants of the 82−146 wild-type subunit [PrP-$(82-146)_{wt}$] were also examined, including entirely, [PrP-$(82-146)_{scr}$], and partially scrambled, [PrP-$(82-146)_{106-126scr}$] and [PrP-$(82-146)_{127-146scr}$], peptides. Al^{3+} strongly stimulated the conversion of native hPrP into the altered conformation, and its potency in inducing aggregation was very high. Despite a lower rate and extent of prion protein conversion into altered isoforms, however, Zn^{2+} was more efficient than Al^{3+} in promoting organization of hPrP aggregates into well-structured, amyloid-like fibrillar filaments, whereas Mn^{2+} delayed and Cu^{2+} prevented the process. GSS peptides underwent the fibrillogenesis process much faster than the full-length protein. The intrinsic ability of PrP-$(82-146)_{wt}$ to form fibrillar aggregates was exalted in the presence of Zn^{2+} and, to a lesser extent, of Al^{3+}, whereas Cu^{2+} and Mn^{2+} inhibited the conversion of the peptide into amyloid fibrils. Amino acid substitution in the neurotoxic core (sequence 106−126) of the 82−146 fragment reduced its amyloidogenic potential. In this case, the stimulatory effect of Zn^{2+} was lower as compared to the wild-type peptide; on the contrary Al^{3+} and Mn^{2+} induced a higher propensity to fibrillation, which was ascribed to different binding modalities to GSS peptides. In all cases, alteration of the 127−146 sequence strongly inhibited the fibrillogenesis process, thus suggesting that integrity of the C-terminal region was essential both to confer amyloidogenic properties on GSS peptides and to activate the stimulatory potential of the metal ions.

The post-translational modification of the prion protein from a normal cellular isoform (PrP^C)[1] to disease specific species (PrP^{Sc}) is the molecular signature of the prion-related encephalopathies (PRE). Extracellular PrP amyloid deposits occur consistently in genetic forms of disease, such as Gerstmann−Sträussler−Scheinker (GSS) disease and in the new variant of Creutzfeldt−Jakob disease which is causally linked to bovine spongiform encephalopathy (*1*, *2*). Conversion of the native PrP^C to the aberrant isoform involves a substantial conformational change: PrP^C is a proteinase K sensitive (PK-sensitive), α-helical monomer, whereas PrP^{Sc} is an assembled multimer characterized by enhanced resistance to PK digestion and a great amount (∼ 45−50%) of *β*-structure (*3*−*6*). The mechanisms underlying the PrP^C conversion to PrP^{Sc} and the endogenous or environmental factors contributing to this process are still unclear.

Research over the past years demonstrates that PrP^C selectively binds Cu^{2+} with low micromolar/nanomolar affinity by coordinating the metal to the HGGGW units of the octapeptide repeats in the N-terminal domain. This finding, associated with other observations, has led to the proposal of a possible physiological role of PrP^C in Cu^{2+} metabolism (*7*−*16*).

In addition to its physiological function, copper is believed to play an important role in the pathogenesis of prion diseases. The N-terminal portion encompassing the octarepeat region is not critical for transmission of prions (*17*, *18*), thus suggesting that Cu^{2+} binding to this area may not be essential for PrP^C conversion to PrP^{Sc}. However, recently Cu^{2+}-binding sites have been found in the C-terminus as well, including His-96 and His-111. Binding of Cu^{2+} to PrP regions alternative to the octarepeat domain may affect the pathways

† This work was supported by a grant from CNR/MIUR (FIRB No. RBNE03PX83).

* Author to whom correspondence should be addressed. Mailing address: CNR Institute of Biomedical Technologies, Metalloproteins Unit, Department of Biology, University of Padova, Viale G. Colombo 3, 35121 Padova, Italy. Tel: 39-049-8276331. Fax: 39-049-8276348. E-mail: zatta@mail.bio.unipd.it.

‡ Department of Biology, University of Padova.

§ Institute of Pharmacological Researches "Mario Negri".

|| Department of Biological Chemistry, University of Padova.

[1] Abbreviations: AD, Alzheimer's disease; Ala, alanine; ANS, 8-anilinonaphthalene-1-sulfonic acid; CAA, cerebral amyloid angiopathy; CJD, Creutzfeldt−Jacob disease; Gly, glycine; GSS, Gerstmann−Sträussler−Scheinker; His, histidine; hPrP, human prion protein; Leu, leucine; PK, proteinase K.; PrP^C, cellular prion protein; PrP^{Sc}, scrapie prion protein; PK, proteinase K.; SHaPrP, Syrian hamster prion protein; TEM, transmission electron microscopy; ThT, thioflavin.

10.1021/bi0601454 CCC: $33.50
Published on Web 05/05/2006

of misfolding and, therefore, impact the physical properties of amyloid fibrils generated in vitro (*19*−*29*). Thus, binding of Cu^{2+} to anomalous sites was reported to convert the protein into a partially PK-resistant state (*26*−*28*) and induce β-sheet formation in the amyloidogenic region of the molecule (*25*, *29*). In contrast with these observations, the presence of Cu^{2+} was shown to inhibit in vitro conversion of prion protein into amyloid fibrils (*30*, *31*), to reduce the accumulation of PrP^{Sc} in scrapie-infected neuroblastoma cells and to delay prion disease propagation in scrapie-infected animals (*32*). In a thorough study aimed at better defining the interaction properties of Cu^{2+} and PrP, Bocharova et al. (*31*) proposed a model which can explain the contradictory data reported in the literature. Depending on the circumstances, Cu^{2+} can exert opposing effects on PrP. It can prevent the conversion of native PrP into the aberrant isoform by stabilizing a nonamyloidogenic PK-resistant form of the protein; on the other hand, it can also enhance the PK-resistance of preformed fibrils and induce their aggregation into large clamps. Taken together, these findings suggest that the potential effect of Cu^{2+} on the pathogenesis of prion diseases is complex and might be mediated through metal interaction with both normal and disease-specific isoforms of PrP (*31*).

Other bivalent metal ions such as Mn^{2+} and Zn^{2+} were shown to induce defective conformational rearrangements of PrP^{C} that could trigger neurotoxicity and affect formation and propagation of PrP^{Sc} aggregates in vivo (*25*, *33*, *34*). Along these lines, aberrantly high levels of Zn^{2+} and Mn^{2+}, which were absent in the healthy controls, were found colocalized with PrP^{Sc} in the brain tissues of subjects affected by Creutzfeldt−Jacob disease (CJD) (*35*).

On this basis, we believe that the involvement of certain metal ions in the etiopathogenesis of the prion diseases could be very important, similarly to what has been postulated for other neurodegenerative disorders, including Alzheimer's disease (AD) (*36*−*38*).

In this study, we investigated the effects of Cu^{2+}, Mn^{2+}, Zn^{2+}, and Al^{3+} on the biophysical properties of the recombinant human prion protein (hPrP). The choice of Al^{3+} in addition to the bivalent ions was based on recent observations that Al^{3+} was highly efficient in stimulating the spontaneous aggregation/fibrillogenesis of Aβs, the cytotoxic species involved in AD (*37*). The research was extended to the fragment of PrP spanning residues 82−146, which was identified as a major component in the brain of patients affected by GSS disease (*39*−*41*). Variants of the 82−146 wild-type subunit [PrP-$(82-146)_{wt}$] were also examined, including entirely, [PrP-$(82-146)_{scr}$], and partially scrambled, [PrP-$(82-146)_{106-126scr}$] and [PrP-$(82-146)_{127-146scr}$], peptides. Both regions spanning residues 102−126 and 127−147 were shown to be crucial for amyloid fibril formation (*42*).

MATERIALS AND METHODS

Recombinant Full-Length Human Prion Protein (hPrP) and GSS Peptides. hPrP was obtained by DNA recombinant techniques. The sequence encoding human prion protein (23−230) (hPrP-(23−230)) was amplified by PCR using human placenta DNA as template and the following primers: 5′ ATGGATCCAAGAAGCGCCCGAAGCCTGGAGGATG 3′ and 5′ GAGAATTCACGATCCTCTCTGGTAATAGGCC 3′. The amplified product was cloned in pRSETA plasmid (Invitrogen) between *Bam*HI and *Eco*RI restriction sites, whereby the residue amino acid sequence of PrP was N-terminally fused to a sequence encoding for a polyhistidine tag and a thrombin cleavage site. The plasmid was verified by double-stranded DNA sequencing (ABI prism kit, Applied Biosystem, Foster City, CA). Expression and purification of hPrP was carried out as described previously (*21*). Purified hPrP was confirmed by SDS−PAGE, RP-HPLC, and electron mass spectrometry, with the presence of an internal disulfide bridge. Circular dichroism showed that the protein was predominantly in α-helical structure.

The following peptides were chemically synthesized and purified according to the procedure described previously (*20*, *43*): PrP-(82−146) wild-type, PrP-$(82-146)_{wt}$, GQPHGGGWGQGGGTHSQWNKPSKPKTNMKHMAGAAAAGAVVGGLGGYMLGSAMSRPIIHFGSDYE; PrP-$(82-146)_{106-126scr}$ with a scrambled sequence in the region spanning residues 106−126, GQPHGGGWGQGGGTHSQWNKPSKP**NGAKALMGGHGATKVMVGAAA**GYMLGSAMSRPIIHFGSDYE; PrP-$(82-146)_{127-146scr}$ with a scrambled sequence in the region spanning residues 127−146, GQPHGGGWGQGGGTHSQWNKPSKPKTNMKHMAGAAAAGAVVGGLG**SMYPASHGLMEDFYGIGSIR**; PrP-$(82-146)_{scr}$ with a totally scrambled sequence, **EADQFALGGSKHGNGMQQVAGHGGSMGAKAWGANGHPSGTGIPTAKMVPYKIYGGGWAGMGRPSS**.

Chemicals. Thioflavin T (ThT), 8-anilinonaphthalene-1-sulfonic acid (ANS), $ZnCl_2$, $MgCl_2$, $Al(C_3H_5O_3)_3$, and $CuSO_4$ were purchased from Sigma-Aldrich Chemical Co. (St. Louis, MO). $Al(C_3H_5O_3)_3$ was used instead of Al^{3+} inorganic salts in order to improve the metal soluble concentrations (*44*). The complex was purified and stored according to the protocol reported by Zatta et al. (*45*). All other chemicals were of the purest analytical grade.

Preparation of hPrP and GSS Peptide Solutions. Solutions of full-length protein and GSS peptides at 1. 3 μM concentration were freshly prepared in 0.1 M Tris/HCl buffer plus 150 mM NaCl (pH = 7.4) (standard medium), at T = 25 °C, unless otherwise specified. To study the effects of metal ions, 50 μM Cu^{2+}, Mn^{2+}, Zn^{2+}, and Al^{3+} were added to 1.3 μM protein/peptide solutions The concentration of metal ions to be used was determined after following the changes of the hPrP/GSS peptide intrinsic (tryptophan) fluorescence as a function of increasing metal amounts: depending on the nature of metal and/or PrP, tryptophan emission was not further affected after addition of a 20−38-fold excess of metal (data not shown).

The levels of metal contamination in the buffers with no added metals were assayed by atomic absorption spectroscopy. In all buffer preparations, metal traces were below the detection limit.

ANS and ThT Binding to hPrP and GSS Peptides. hPrP and GSS peptides at 1.3 μM in the standard medium, both in the absence and in the presence of added metals (50 μM Cu^{2+}, Mn^{2+}, Zn^{2+}, and Al^{3+}), were left to incubate for 5 min before addition of ANS (6.5 μM).

ANS binding to the different protein/peptides was followed by the increase of fluorescence emission of ANS in the range 400−700 nm (λ_{exc} = 360 nm).

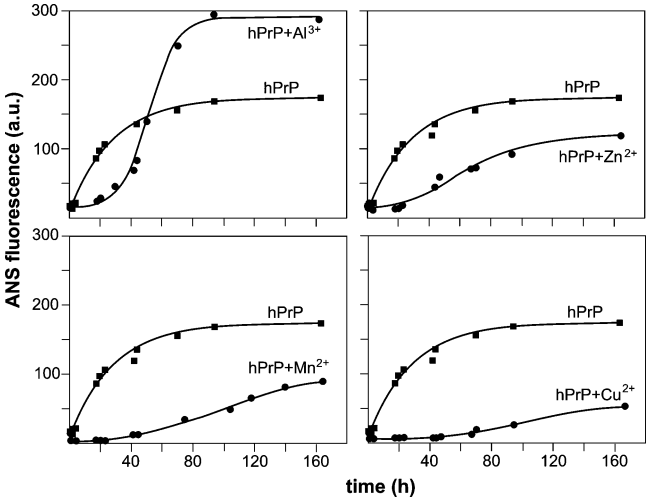

FIGURE 1: Time course of surface hydrophobicity of hPrP, both in the absence and in the presence of added Al^{3+}, Zn^{2+}, Mn^{2+}, and Cu^{2+}, as monitored by the ANS fluorescence changes. The ANS fluorescence is reported as the area of the emission spectra (in the range 370−700 nm; λ_{exc} = 360 nm) after subtraction of the free dye (or free dye plus metals) contribution. Freshly prepared solutions of hPrP alone (1.3 μM) and hPrP plus metals (50 μM) in 0.1 M Tris/HCl buffer plus 150 mM NaCl (pH = 7.4) were left to incubate for 5 min at T = 25 °C before addition of ANS (6.5 μM).

ThT (5 μM) binding was followed by the increase of fluorescence intensity at 445 nm with excitation at 385 nm under the same experimental conditions used in ANS studies.

The fluorescence measurements were performed with a Perkin-Elmer LS 50B spectrophotofluorimeter equipped with a thermostatic cell holder and magnetic stirring.

Transmission Electron Microscopy (TEM) Measurements. hPrP and GSS peptides at 13 μM concentrations in the standard medium were incubated for different periods of time (15−30 days) at 37 °C in the absence and in the presence of added metals (130 μM Al^{3+}, Mn^{2+}, Zn^{2+}, and Cu^{2+}). Experiments at 4 °C were also carried out for hPrP. Diluted aliquots of the preparations were absorbed onto glow-discharged carbon-coated Formwar films on 400-mesh copper grids. The grids were negatively stained with 1% uranyl acetate and observed at 40000× by TEM (Hitachi H600).

RESULTS

Changes in Surface Hydrophobicity of hPrP and GSS Peptides and Stimulation by Metal Ions. Aggregation of proteins/peptides is generally preceded by conformational changes of the monomers which lead to solvent exposure of the molecule hydrophobic core. Subsequently, intermolecular hydrophobic interactions cause the monomers to stack and generate structured polymers. Formation of surface hydrophobic clusters can be sensed by following the changes in the ANS fluorescence properties, such as the increment in emission intensity and the blue shift of the emission maximum (*46*). Binding of ANS to the full-length protein and the various PrP 82−146 peptides was followed over a period of 160 h.

Figure 1 shows a typical time course of the changes in ANS fluorescence emission after dye interaction with hPrP, and the effects of the various metal ions added. ANS fluorescence is expressed as the area of the emission spectra of protein-bound ANS after subtraction of the free dye (or free dye plus metals) contribution. As deduced by the ANS spectral changes, hPrP spontaneously exposes hydrophobic patches with a relatively fast kinetics (within 40 h). In the presence of all metal ions under examination an induction lag phase is observed, with duration depending on the nature of the metal. The full process appears to be strongly stimulated by Al^{3+}, whereas it is considerably inhibited by Cu^{2+} and, to a lesser extent, by Mn^{2+} and Zn^{2+}.

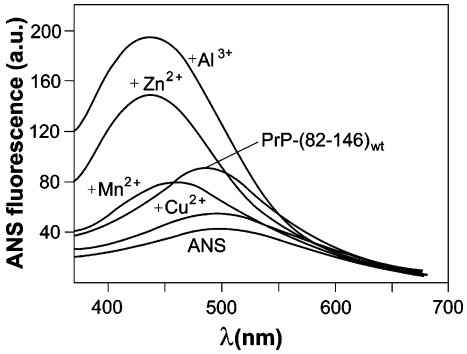

FIGURE 2: Fluorescence emission spectra of ANS before and after interaction with PrP-$(82-146)_{wt}$, both in the absence and in the presence of added Al^{3+}, Zn^{2+}, Mn^{2+}, and Cu^{2+}. The ANS emission spectra (λ_{exc} = 360 nm) were collected after 160 h incubation of the dye with the peptide. Freshly prepared solutions of PrP-$(82-146)_{wt}$ alone (1.3 μM) and PrP-$(82-146)_{wt}$ plus metals (50 μM) in 0.1 M Tris/HCl buffer plus 150 mM NaCl (pH = 7.4) were left to incubate for 5 min at T = 25 °C before addition of ANS (6.5 μM).

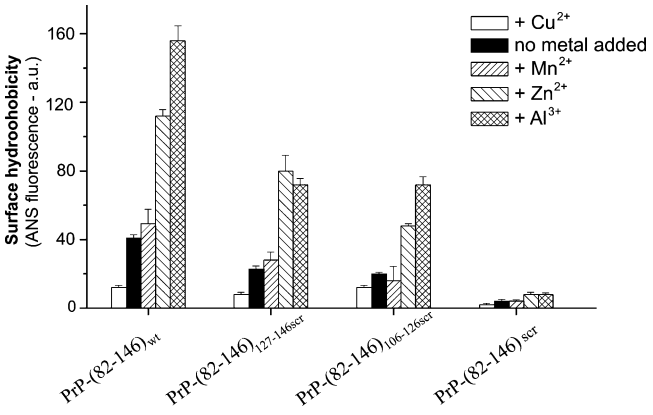

FIGURE 3: Changes in surface hydrophobicity of PrP-$(82-146)_{wt}$ induced by sequence alterations, both in the absence and in the presence of added Al^{3+}, Zn^{2+}, Mn^{2+}, and Cu^{2+}. The peptide surface hydrophobicity after 160 h incubation is expressed as the area of the emission spectra of peptide-bound ANS after subtraction of the free dye (or free dye plus metals) contribution. The experimental conditions were the same as those reported in the caption to Figure 2. The data are the average of three independent determinations. Error bars represent ± standard deviation.

Figure 2 shows the spectral changes of ANS emission after 160 h incubation with the GSS fragment PrP-$(82-146)_{wt}$, both in the absence and in the presence of added metals (Al^{3+}, Zn^{2+}, Mn^{2+}, and Cu^{2+}). For a better comparison, the spectrum of the free dye is also reported. It is clearly evidenced that both the increase in ANS emission intensity and blue-shift of the emission maximum follow the order $Al^{3+} > Zn^{2+} >$ no metal added $\cong Mn^{2+} \gg Cu^{2+}$.

The changes in surface hydrophobicity induced by sequence alterations of the wild-type peptide, as sensed by the ANS fluorescence changes, are reported in Figure 3. Some differences in the ability of metal ion to induce structural

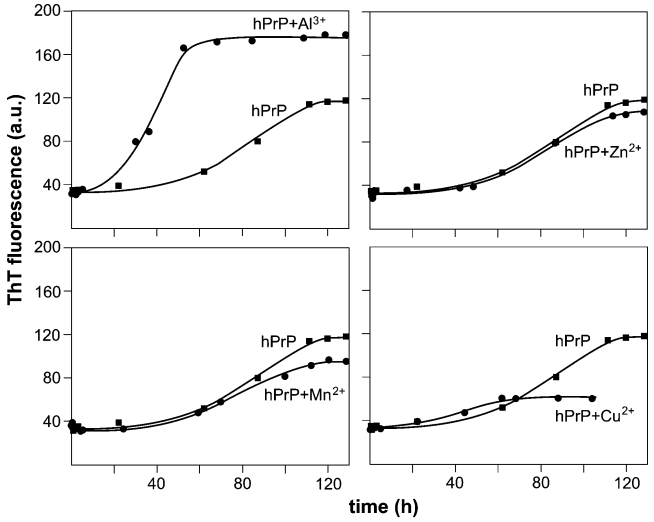

FIGURE 4: Time course of hPrP aggregation both in the absence and in the presence of added Al^{3+}, Zn^{2+}, Mn^{2+}, and Cu^{2+}. Aggregation kinetics were sensed by the ThT fluorescence variations at 445 nm (λ_{exc} at 385 nm). The fluorescence intensity is given after subtraction of the free dye (or free dye plus metals) contribution. Freshly prepared solutions of hPrP alone (1.3 μM) and hPrP plus metals (50 μM) in 0.1 M Tris/HCl buffer plus 150 mM NaCl (pH = 7.4) were left to incubate for 5 min at $T = 25$ °C before addition of ThT (4 μM).

perturbation can be noticed in scrambled peptides, as compared to the native sequence; in particular, PrP-(82−146)$_{127-146scr}$ is affected to a greater degree by Zn^{2+} rather than by Al^{3+}. In general, sequence alterations reduce the metal-induced conformational modifications up to full inhibition for totally scrambled peptide. The reduction in surface hydrophobicity appears to be due to intrinsic structural characteristics of the different peptides, rather than to metal binding, since an analogous trend was observed in the absence of added metal ions.

Aggregation of hPrP and GSS Peptides and Stimulation by Metal Ions. Formation of amyloidogenic protein/peptide aggregates can be sensed by following the changes in the ThT fluorescence properties, such as the increment in emission intensity at 445 nm (excitation at 385 nm), typical of the free dye, and appearance of a new excitation band peaking at 450 nm with enhanced emission at 482 nm. These changes are dependent on the aggregation state, as monomeric or dimeric forms do not enhance the ThT fluorescence (*47*).

Binding of ThT to the full-length protein and the PrP 82−146 peptides was followed over a period of 130 h under the same experimental protocol used for ANS binding. Since protein concentration was extremely low (1.3 μM), the emission band at 482 nm was weak and only the emission at 445 nm was considered.

Figure 4 shows an example of aggregation kinetics of hPrP, both in the absence and in the presence of added metal ions. Under our experimental conditions, hPrP exhibits an intrinsic tendency to polymerize. The conversion process develops in a time interval of about 130 h and displays a lag phase of about 60 h. Aggregation is substantially unaffected by Mn^{2+} and Zn^{2+}, whereas it is inhibited by Cu^{2+}, as judged by the negligible increase in ThT fluorescence. The noticeable shortening of the lag phase and increment of ThT emission suggest that Al^{3+} is very efficient

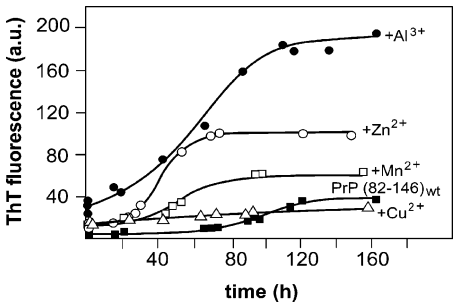

FIGURE 5: Time course of PrP-(82−146)$_{wt}$ aggregation both in the absence and in the presence of added Al^{3+}, Zn^{2+}, Mn^{2+}, and Cu^{2+}, as followed by the ThT fluorescence at 445 nm (λ_{exc} at 385 nm). The fluorescence intensity is given after subtraction of the free dye (or free dye plus metals) contribution. Freshly prepared solutions of PrP-(82−146)$_{wt}$ alone (1.3 μM) and PrP-(82−146)$_{wt}$ plus metals (50 μM) in 0.1 M Tris/HCl buffer plus 150 mM NaCl (pH = 7.4) were left to incubate for 5 min at $T = 25$ °C before addition of ThT (4 μM).

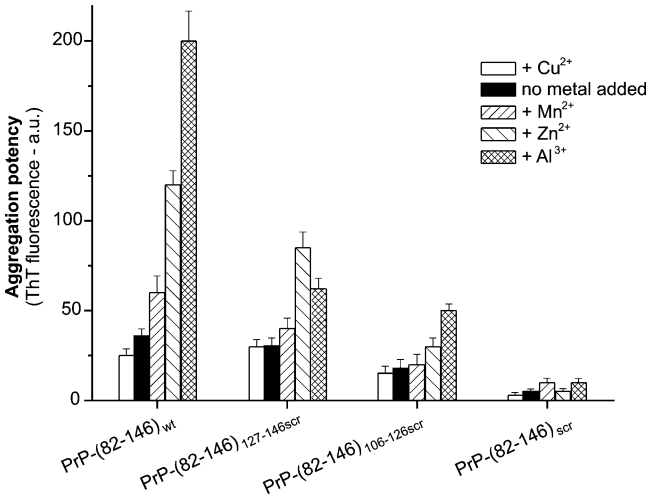

FIGURE 6: Comparison between the aggregation potencies of PrP-(82−146)$_{wt}$, PrP-(82−146)$_{127-146scr}$, PrP-(82−146)$_{106-126scr}$, and PrP-(82−146)$_{scr}$, both in the absence and the presence of added Al^{3+}, Zn^{2+}, Mn^{2+}, and Cu^{2+}. The peptide aggregation potency after 160 h incubation is expressed as the fluorescence intensity at 445 nm (λ_{exc} at 385 nm) of the peptide-bound ThT after subtraction of the free dye contribution. The experimental conditions were the same as those reported in the caption to Figure 5. The data are the average of three independent determinations. Error bars represent ± standard deviation.

in both accelerating and promoting protein aggregation, in parallel with its higher propensity to induce surface exposure of hydrophobic domains (Figure 1).

Figure 5 illustrates a typical time course of aggregation of PrP-(82−146)$_{wt}$ peptide. It is interesting to notice that in this case Zn^{2+} and Mn^{2+} are able to efficiently promote peptide conversion to amyloidogenic aggregates, in contrast with the effects of the two metals on the full-length PrP. Again, Al^{3+} was the most efficient in stimulating the spontaneous aggregation, whereas Cu^{2+} prevented the process.

The aggregation studies of the different GSS peptides substantially confirm the close relationship between the metal propensity to promote surface exposure of hydrophobic groups (Figure 3) and to induce polymerization (Figure 6). Actually, the potency rank for aggregate formation determined after 160 h incubation follows the same order as for hydrophobic clusters generation; namely, when referred to

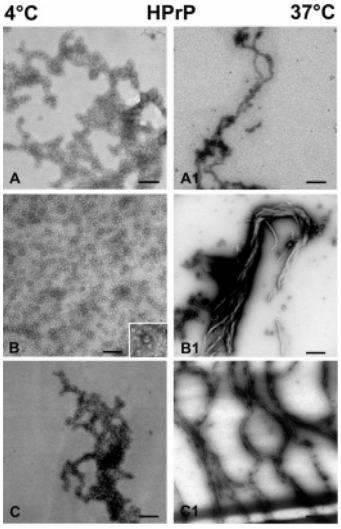

FIGURE 7: Electron micrographs of the aggregates generated by hPrP in the absence and the presence of added metal ions. hPrP and cation concentrations were, respectively, 13 and 130 μM. The micrographs show the structure of the aggregates of hPrP after 30 days' incubation in 0.1 M Tris/HCl buffer plus 150 mM NaCl (pH = 7.4) at 4 °C (A) and 37 °C (A1). Panels B,B1 and C,C1 show the micrographs obtained, respectively, for hPrP plus Al^{3+} or Zn^{2+} under the same experimental conditions.

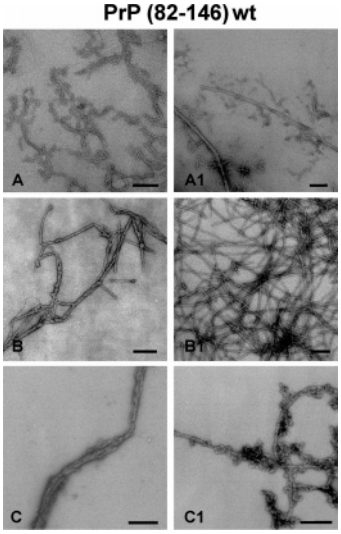

FIGURE 8: Electron micrographs of the aggregates generated by PrP-$(82-146)_{wt}$ in the absence and the presence of added metal ions at 37 °C. The peptide and cation concentrations were 13 and 130 μM. The left and right panels show, respectively, the results obtained after 15 and 30 days' incubation in 0.1 M Tris/HCl buffer plus 150 mM NaCl (pH = 7.4) for PrP-$(82-146)_{wt}$ alone (A, A1) and after addition of Zn^{2+}(B, B1) and Al^{3+}(C, C1).

the fragment type, both in the absence and in the presence of added metal ions, PrP-$(82-146)_{wt}$ > PrP-$(82-146)_{127-146scr}$ ≥ PrP-$(82-146)_{106-126scr}$ ≫ PrP-$(82-146)_{scr}$. In analogy with the results concerning surface hydrophobicity, the metal stimulatory capacity also increases in the order Al^{3+} > Zn^{2+} (with the exception of 127−146 scrambled sequence) ≫ Mn^{2+} ≅ no metal added > Cu^{2+}.

It must be noticed that similar effects on the conformational (ANS test) and aggregational (ThT test) properties of hPrP and GSS peptides were obtained with different metal/protein stoichiometries, the amount of metal only affecting the rate of the conversion processes.

Ultrastructural Analysis of the Aggregates of hPrP and GSS Peptides and Influence of Metal Ions. TEM studies allow us to obtain information on the evolution of prion protein/peptide aggregates to higher, structured polymers. The experimental conditions chosen were more drastic (higher temperatures, 37 °C, and hPrP/GSS peptide concentrations, 13 μM) than those previously used, in order to accelerate the prion structural organization. Samples of hPrP were analyzed also at 4 °C, to evidence the presence of oligomers, possible precursors of the final structure.

The electron micrographs show that the full-length hPrP after 30 days at 4 °C generates primarily a dense population of small oligomers with spherical and annular shape. These oligomers are clearly distinguishable in the presence of Al^{3+} (Figure 7B), whereas they adhere to each other to form agglomerates in the case of non-metal-supplemented hPrP and Zn^{2+}-containing hPrP (Figure 7A,C). A large amount of short, irregular protofibrils together with few, long filaments can be observed in hPrP in the absence of added metals after incubation for 30 days at 37 °C (Figure 7A1). Conversely, rather long and paired fibrils were formed after addition of Al^{3+} and Zn^{2+} (Figure 7B1,C1). Annular oligomers together with a small population of very short protofibrils can be evidenced with Mn^{2+}, whereas no definite structure was observed with Cu^{2+} (not shown).

TEM studies have been extended to PrP-$(82-146)_{wt}$, PrP-$(82-146)_{127-146scr}$, and PrP-$(82-146)_{106-126scr}$ peptides, which exhibit a decreasing order of propensity for aggregation (Figure 6), whereas totally scrambled peptide was not examined.

The electron micrographs of PrP-$(82-146)_{wt}$ in the absence of added metal ions after 15 days' incubation at 37 °C evidenced the formation of short fibrillar filaments (Figure 8A), which did not evolve significantly over 30 days' incubation (Figure 8A1). After addition of Cu^{2+} and Mn^{2+}, shapeless and small polymers were present (not shown). On the contrary, addition of Zn^{2+} to PrP-$(82-146)_{wt}$ induced the formation of long and branched filaments (Figure 8B), which generate a dense network of deeply branched fibrils after 30 days' incubation (Figure 8B1). In the presence of Al^{3+}, the mature fibrillar filaments appear greatly elongated and laterally coupled as shown after 15 (Figure 8C) and 30 days (Figure 8C1). Numerous oligomeric annular precursors attached to the mature filaments could also be observed (Figure 8C1).

PrP-$(82-146)_{127-146scr}$ and PrP-$(82-146)_{106-126scr}$ peptides were analyzed only after 30 days at 37 °C. The results are shown in Figure 9. In the absence of added metal ions, modification of the sequence 106−126 in the peptide leads to the formation of relatively few amyloid fibrils (Figure 9A) together with large amounts of very short protofibrils. The density of fibrillar assemblies increases considerably after addition of Mn^{2+} (B), Zn^{2+} (C), and Al^{3+}(D), whereas Cu^{2+} does not affect the spontaneous peptide fibrillogenesis significantly (not shown). Despite the higher propensity to aggregate of PrP-$(82-146)_{127-146scr}$ (see ThT fluorescence, Figure 6), as compared to PrP-$(82-146)_{106-126scr}$, alteration of the 127−146 region generated primarily amorphous material associated with few, relatively short, unbranched, irregular filaments in all cases (Figure 9A1−D1).

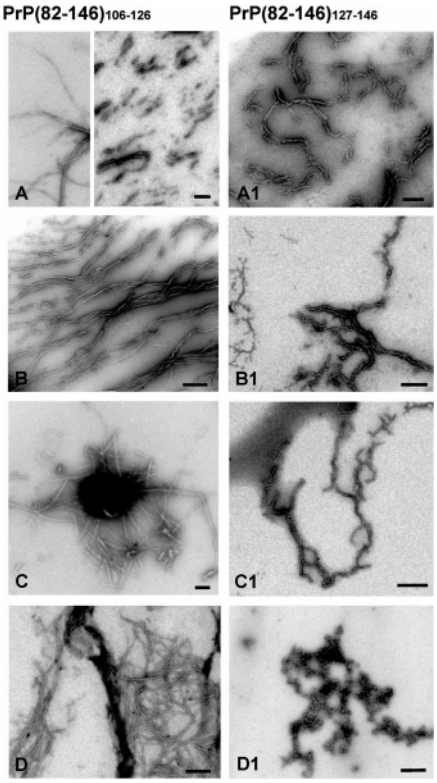

FIGURE 9: Electron micrographs of the aggregates generated by PrP-(82−146)$_{106-126scr}$ (left) and PrP-(82−146)$_{126-147scr}$ (right) after 30 days at 37 °C. The experiments were carried out in the absence of added metals (A, A1), and after addition of Mn^{2+} (B, B1), Zn^{2+} (C, C1), and Al^{3+} (D, D1). The peptide and metal concentrations were, respectively, 13 and 130 μM in 0.1 M Tris/HCl buffer plus 150 mM NaCl (pH = 7.4).

DISCUSSION

Disturbances in the levels of metal ions, namely, Cu^{2+}, Zn^{2+}, and Mn^{2+}, have been described in prion-infected brain tissues (*35*, *48*). On this basis, it has been postulated that binding of metal ions might modulate the structure and function of PrP^C, and directly influence its structural conversion to PrP^{Sc} and the formation of amyloid aggregates. On the other hand, a large body of data has already demonstrated that metal ions, in particular Cu^{2+}, Fe^{3+}, Zn^{2+}, and Al^{3+}, modulate the conversion to amyloid fibrils and the toxicity of Aβs, the peptides involved in AD (*36*, *37*). These findings have stimulated in vitro studies aimed at investigating whether this property was common to other amyloidogenic molecules, including PrP. Studies of the effects induced by metal ions on PrP structure should be of particular significance, since it has been shown that the neurotoxic core of the prion molecule (residues 106−126) exhibits surprising analogies in some physicochemical properties with Aβ_{1-40} and Aβ_{1-42}, the most representative Aβ peptides of AD (*25*, *49*).

Whereas the influence of Cu^{2+} on the biophysical behavior of PrP and of different fragments of PrP has been extensively studied (*23*−*31*, *33*), there are only few reports on the effects of Zn^{2+} and Mn^{2+} and, to the best of our knowledge, no data on the effect of Al^{3+}. Al^{3+} is a well-known neurotoxic metal ion that causes cognitive deficiency and dementia when it enters the brain. It has long been recognized as a neurotoxic element in many biological models and repeatedly associated with the etiopathology of several neurological disorders, such as encephalopathies in long-term hemodialysis, amyotrophic lateral sclerosis, Parkinsonism dementia, and AD (*44*, *46*, *50*). Al^{3+} concentrations between 1.4 and 17.5 ppm (dry weight) have been measured in normal human brain (*51*). A considerable increase in aluminum content in the lesioned brain areas of patients affected by different neurodegenerative disorders (*46*, *51*) was observed when compared with control tissues.

In vitro studies have revealed that a crucial effect of Al^{3+} is to efficiently promote misfolding/aggregation of several neurological disease related proteins, such as β-amyloids of AD (*37*, *50*) and α-synuclein of Parkinson disease (*46*). In the present study we planned to investigate whether similar effects could be observed for PrP and their extent was comparable to those due to Mn^{2+}, Cu^{2+}, and Zn^{2+}.

We used recombinant PrP which was proven to be a valuable biophysical model for elucidating structural aspects of the prion replication (*52*). The research was extended to PrP fragments spanning residues 82−146. It is known that the conformational conversion leading to PrP amyloidogenesis occurs to the highest degree in the genetically determined GSS and prion protein cerebral amyloid angiopathy (PrP-CAA), while it is less frequently seen in other prion diseases (*53*). Fragments spanning residues 81−82 to 140−153, such as PrP-(82−146), mainly account for the massive deposition of PrP amyloid in GSS and CAA (*39*, *40*, 53). Interestingly, these fragments are an integral part of the minimal sequence which sustains prion replication (*54*−*56*), and play a central role in the conformational transition of PrP^C into PrP^{Sc} and in PrP^{Sc} propagation (*57*). On this basis, wild-type and modified peptides spanning 82−146 residues can be conveniently used for testing compounds, including metals, capable of binding to this critical domain and stabilizing or destabilizing the PrP structurally altered isoforms.

The results obtained following ANS and ThT fluorescence clearly show that, at neutral pH, the aggregation process of full-length hPrP is efficiently inhibited by Cu^{2+} and substantially unaffected by Mn^{2+} and Zn^{2+} (Figure 4), even though the latter metal ions retard the formation of the hPrP misfolded conformation (Figure 1). In striking contrast with the bivalent metal ions, Al^{3+} strongly stimulates the conversion of native hPrP into the altered conformation (Figure 1) and its potency in inducing aggregation is very high (Figure 4). ANS- and ThT-based tests, however, do not unambiguously demonstrate that misfolded aggregates are amyloidogenic: actually, TEM examination shows that Zn^{2+} is even more efficient than Al^{3+} in promoting organization of hPrP aggregates into well-structured, amyloid-like fibrillar filaments (Figure 7), despite the large difference in the rate and extent of prion protein conversion to altered isoforms. Under the same experimental conditions, Mn^{2+} delays and Cu^{2+} prevents the process.

The data obtained with Cu^{2+} are consistent with previous observations also reporting that this metal ion prevents in vitro the prion fibrillogenesis process at pH > 7 (*30*, *31*, *33*). The inhibitory effect of Cu^{2+} was assigned to the highly selective binding of Cu^{2+} to the octarepeat region of monomeric PrP. This binding results in a less flexible N-terminus which is compatible with oligomer formation but prevents the association of oligomers into larger aggregates by sterical hindrance (*33*). Inhibition of PrP polymerization by Mn^{2+} and Zn^{2+} is less or not efficient probably because

binding of these metal ions to the octarepeats displays much lower affinity, compared to copper (*31*).

TEM studies at low temperature indicate that the possible precursors of the hPrP amyloid fibrils, which are formed in the early stages of the aggregation process, consist of small structures of spherical and annular shape. These structures are clearly distinguishable in the presence of Al^{3+} (Figure 7B) whereas they are associated in agglomerates in hPrP alone and after addition of Zn^{2+} (Figure 7A,C). The spherical oligomers can be correlated to similar forms observed by Sokolowsky et al. (*58*) for the recombinant Syrian hamster prion protein (SHaPrP). In the opinion of these authors, they are formed by eight monomeric units and could represent the critical precursors obtained during the conformational transition of native PrP to its aberrant isoform. While the circular oligomeric precursors of SHaPrP have been observed only at acidic pH and low protein concentration, our results indicate that they can be evidenced also at physiological pH and higher PrP concentrations if the aggregation process is slowed by low temperatures.

The results obtained for the fragments spanning residues 82−146 of prion protein demonstrate that elimination of most of the octarepeat region makes available additional, high-affinity, metal binding sites that are probably masked in the full-length protein. This is particularly evident for Zn^{2+}; actually, the complexes of Zn^{2+} with PrP 82−146 fragments have the highest propensity to assemble into large clumps of branched fibrillar filaments (Figures 8B, 9C) that are ultrastructurally similar to those observed in GSS patients. The onset of aggregation and neurotoxicity of Zn^{2+}-containing defective prion protein has previously been associated with binding of the metal ion to an anomalous site comprising His-111 (*25*). In agreement with this, alteration of the amino acid sequence in the 106−126 region and replacement of His-111 with Leu reduces the process of amyloid fibril generation (Figures 8, 9). However, since fibrillation is not abolished, the role of additional His such as His-96 and/or His-140 as determinant Zn^{2+}-binding sites cannot be ruled out.

Binding sites alternative to the octarepeat domains and comprising His-96 and His-111, which could become accessible to the metal in the altered PrP^{C} isoform, have been postulated also for Cu^{2+} (*19*−*25*). Cu^{2+} binding to these anomalous sites has been reported to convert the native prion protein to a partially PK resistant state (*26*−*28*) and induce β-sheet formation in the amyloidogenic neurotoxic core of the molecule (*25*, *29*). On the contrary, our results show that Cu^{2+} inhibits conversion of both full-length and truncated protein into amyloid fibrils. The lack of Cu^{2+} proaggregating activity in PrP 82−146 fragments could be due to a preferential binding of the metal to the residual His-octarepeat domain. According to Bocharova et al. (*31*), however, Cu^{2+}-dependent inhibition occurs even in the absence of the octarepeat region, due to the stabilization by copper of a nonamyloidogenic form of PrP.

It has been reported that Mn^{2+} ions amplify full-length prion protein aggregation (*25*, *30*, *33*, *34*) and promote fibril generation in solution (*59*). Thus, Mn^{2+}-loaded PrP may contribute to the formation of the pathogenic isoform of PrP (*60*). The proaggregating Mn^{2+} effects are apparently due to metal binding on sites of preformed altered PrP that do not require His, whereas native PrP is not affected (*33*, *61*). Qualitative information on carbonyl oxygens of Gly-124 and Leu-125 as Mn^{2+}-binding sites at acidic pH has been obtained recently (*62*). In contrast, our results indicate that Mn^{2+}-induced aggregation and fibrillation are especially evident for 106−126 scrambled peptide where Gly-124 and Leu-125 have been replaced by Ala (Figure 9B). It is likely that both alkaline pH and/or a different conformational status lead to the unmasking of alternative metal ion binding sites on the prion fragment.

Al^{3+} binding modalities to neurodegenerative protein/peptides have not yet been clarified. Studies on model sequences, however, indicate that Al^{3+} presumably interacts with carboxylate groups of glutamic and aspartic amino acid residues and with −OH of serine (*37*, *63*). At variance with what was observed for β-amyloid, Al^{3+} preferentially favors the structural arrangement of prion protein/peptides to elongated and little branched fibrillar forms and its amyloidogenic potency is lower than that shown by Zn^{2+}.

The comparison between entirely and partially scrambled GSS peptides confirms previous reports indicating that integrity of the C-terminal region is essential for endowing the peptides with amyloidogenic properties (*57*). Actually, the amyloidogenic potential of (82−146)-$PrP_{(127-146)}$ is much lower than that of both (82−146)-$PrP_{(106-126)}$ and (82−146)-PrP_{wt} and is not significantly increased after addition of metals (Figure 9). On the other hand, changes in the sequence 106−126 reduce the density of fibrillar agglomerates induced by Zn^{2+}, whereas the opposite effect is observed with Al^{3+} and Mn^{2+}. This indicates that Al^{3+}- and Mn^{2+}-binding sites in the neurotoxic core of the prion protein/peptides are not critical for fibrillogenesis stimulation, while the C-terminal portion is essential for the metals' proaggregation effects.

Our studies support the role of some metal ions in the biophysical behavior and activity of PrP, which could affect the pathogenesis of prion diseases in vivo. In particular, binding of Zn^{2+} and Al^{3+} has important effects on the amyloidogenic process of both full-length protein and GSS peptides whereas binding of Mn^{2+} is effective in stimulating fibril formation only in the fragment 82−146 after alteration of the 106−126 sequence. On the contrary, Cu^{2+} inhibits in all cases both the conversion into disease-specific conformations and protein fibrillogenesis.

The mechanisms by which metal ions stimulate the conversion of neurodegenerative disorder related proteins into misfolded/amyloidogenic aggregates and the rationale for the differences in their effects are not yet available. The hypothesis has been advanced that binding of metal ions may induce protein misfolding by altering the charge density on the molecule. Binding of cations could reduce the negative charge−charge repulsion and thereby allow for a protein structure supporting aggregation (*46*, *64*). If this is the case, the effectiveness of such metal effects would be reinforced by metal binding to specific protein domains. Molecular dynamics simulation of the unfolding of hPrP has indicated that the native protein conformation is mainly preserved by strong electrostatic repulsive interactions between Glu and Asp residues. The stability of the native fold is very subtle and can be strongly disturbed by eliminating even a single negative charge at key positions (*65*). On these bases, preferential binding of Al^{3+} to and neutralization of Glu and Asp negative charges (*63*) could account for the high accelerating and stimulating effect of Al^{3+} on PrP structural

conversion whereas binding of Cu^{2+}, Mn^{2+}, and Zn^{2+} to amino acidic residues diverse from Glu and Asp would be less effective. In particular, high-affinity binding of Cu^{2+} to His of the N-terminus area that is not determinant for the PrP structural conversion would stabilize the protein in the native state (*7*−*16*). In agreement, no major conformational changes of PrP take place at pH 7.4 in the presence of Cu^{2+} (*30*, *31*).

For protein misfolding/aggregation processes in the presence of polyvalent cations, an additional important factor, namely, the potential for cross-linking or bridging between two or more metal-binding groups, should be considered (*46*). Differing geometric and thermodynamic conditions of metal ion complexing may also account for the differences in the conformational/aggregational effects between different divalent cations, as well as between divalent cations and Al^{3+} (*63*). Clearly, more detailed studies are necessary to better understand the complexity of metal ion induced structural reorganization of neurodegenerative disorder related proteins.

ACKNOWLEDGMENT

We thank Silvano Gobbo, Claudio Friso, and Renzo Mazzaro for the excellent technical assistance.

REFERENCES

1. Will, R. G., Ironside, J. W., Zeidler, M., Cousens, S. N., Estibeiro, K., Alperovitch, A., Poser, S., Pocchiari, M., Hofman, A., and Smith, P. G. (1996) A new variant of Creutzfeldt-Jakob disease in the UK, *Lancet 347*, 921−925.
2. Bruce, M. E., Will, R. G. Ironside, J. W., McConnell, I., Drummond, D., Suttie, A., McCardle, L., Chree, A., Hope, J., Birkett, C., Cousens, S., Fraser, H., and Bostock, C. J. (1997) Transmissions to mice indicate that 'new variant' CJD is caused by the BSE agent, *Nature 389*, 498−501.
3. Prusiner, S. B. (1998) Prions, *Proc. Natl. Acad. Sci. U.S.A. 95*, 13363−13383.
4. Caughey, B. W., Dong, A., Bhat, K. S., Ernst, D., Hayes, S. F., and Caughey, W. S. (1991) Secondary structure analysis of the scrapie-associated protein PrP 27−30 in water by infrared spectroscopy, *Biochemistry 30*, 7672−7680.
5. Pan, K. M., Baldwin, M., Nguyen, J., Gasset, M., Serban, A., Groth, D., Mehlhorn, I., Huang, Z., Fletterick, R. J., Cohen, F. E., and Prusiner, S. B. (1993) Conversion of alpha-helices into beta-sheets features in the formation of the scrapie prion protein, *Proc. Natl. Acad. Sci. U.S.A. 90*, 10962−10966.
6. Safar, J., Roller, P. P., Gajdusek, D. C., and Gibbs, C. J., Jr. (1993) Conformational transitions, dissociation, and unfolding of scrapie amyloid (prion) protein, *J. Biol. Chem. 268*, 20276−20284.
7. Millhauser G. L. (2004) Copper binding in the prion protein, *Acc. Chem. Res. 37*, 79−85.
8. Brown, D. R., Wong, B. S., Hafiz, F., Clive, C., Haswell, S. J., and Jones, I. M. (1999) Normal prion protein has an activity like that of superoxide dismutase, *Biochem. J. 344* (Part 1), 1−5.
9. Whittal, R. M., Ball, H. L., Cohen, F. E., Burlingame, A. L., Prusiner, S. B., and Baldwin, M. A. (2000) Copper binding to octarepeat peptides of the prion protein monitored by mass spectrometry, *Protein Sci. 9*, 332−343.
10. Pauly, P. C., and Harris, D. A. (1998) Copper stimulates endocytosis of the prion protein, *J. Biol. Chem. 273*, 33107−33110.
11. Burns, C. S., Aronoff-Spencer, E., Dunham, C. M., Lario, P., Avdievich, N. I., Antholine, W. E., Olmstead, M. M., Vrielink, A., Gerfen, G. J., Peisach, J., Scott, W. G., and Millhauser, G. L. (2002) Molecular features of the copper binding sites in the octarepeat domain of the prion protein, *Biochemistry 41*, 3991−4001.
12. Hornshaw, M. P., McDermott, J. R., and Candy, J. M. (1995) Copper binding to the N-terminal tandem repeat regions of mammalian and avian prion protein, *Biochem. Biophys. Res. Commun. 207*, 621−629.
13. Brown, D. R., Herms, J., Schmidt, B., and Kretzschmar, H. A. (1997) Different requirements for the neurotoxicity of fragment of PrP and amiloid, *Eur. J. Neurosci. 9*, 1162−1169.
14. Stockel, J., Safar, J., Wallace, A. C., Cohen, F. E., and Prusiner, S. B. (1998) Prion protein selectively binds copper(II) ions, *Biochemistry 37*, 7185−7193.
15. Miura, T., Hori-I, A., Mototani, H., and Takeuchi, H. (1999) Raman spectroscopic study on the copper(II) binding mode of prion octapeptide and its pH dependence, *Biochemistry 38*, 11560−11569.
16. Viles, J. H., Cohen, F. E., Prusiner, S. B., Goodin, D. B., Wright, P. E., and Dyson, H. J. (1999) Copper binding to the prion protein: structural implications of four identical cooperative binding sites, *Proc. Natl. Acad. Sci. U.S.A. 96*, 2042−2047.
17. Prusiner, S. B., McKinley, M. P., Bowman, K. A., Bolton, D. C., Bendheim, P. E., Groth, D. F., and Glenner, G. G.(1983) Scrapie prions aggregate to form amyloid-like birefringent rods, *Cell 35*, 349−358.
18. Fischer, M. B., Rülicke, T., Raeber, A., Sailer, A., Moser, M., Oesch, B., Brandner, S., Aguzzi A., and Weissmann, C. (1996) Prion protein (PrP) with amino-proximal deletions restoring susceptibility of PrP knockout mice to scrapie, *EMBO J. 15*, 1255−1264.
19. Forloni, G., Angeretti, N., Chiesa, R., Monzani, E., Salmona, M., Bugiani, O., and Tagliavini, F. (1993) Neurotoxicity of a prion protein fragment, *Nature 362*, 543−546.
20. De Gioia, L., Selvaggini, C., Ghibaudi, E., Diomede, L., Bugiani, O., Forloni, G., Tagliavini, F., and Salmona, M. (1994) Conformational olymorphism of the amyloidogenic and neurotoxic peptide homologous to residues 106−126 of the prion protein, *J. Biol. Chem. 269*, 7859−7862.
21. Cereghetti, G. M., Negro, A., Vinck, E., Massimino, M. L., Sorgato, M. C., Van Doorslaer S.(2001) Copper(II) binding to the human Doppel protein may mark its functional diversity from the prion protein, *J. Biol. Chem. 279*, 36497−503.
22. Jackson, G. S., Murray, I., Hosszu, L. L., Gibbs, N., Waltho, J. P., Clarke, A. R., and Collinge, J. (2001) Location and properties of metal-binding sites on the human prion protein, *Proc. Natl. Acad. Sci. U.S.A. 98*, 8531−8535.
23. Qin, K., Yang, Y., Mastrangelo, P., and Westaway, D. (2002) Mapping Cu(II) binding sites in prion proteins by diethyl pyrocarbonate modification and matrix-assisted laser desorption ionization-time of flight (MALDI-TOF) mass spectrometric footprinting, *J. Biol. Chem. 277*, 1981−1990.
24. Burns, C. S., Aronoff-Spencer, E., Legname, G., Prusiner, S. B., Antholine, W. E., Gerfen, G. H., Peisach, J., and Millhauser, G. I. (2003) Copper coordination in the full-length, recombinant prion protein, *Biochemistry 42*, 6794−6803.
25. Jobling, M. F., Huang, X., Stewart, L. R., Barnham, K. J., Curtain, C., Volitakis, I., Perugini, M., White, A. R., Cherny, R. A., Masters, C. L., Barrow, C. J., Collins, S. J., Bush, A. I., and Cappai, R. (2001) Copper and zinc binding modulates the aggregation and neurotoxic properties of the prion peptide PrP106-126, *Biochemistry 40*, 8073−8084.
26. Qin, K., Yang, D. S., Yang, Y., Chishti, M. A., Meng, L. J., Kretzschmar, H. A., Yip, C. M., Fraser, P. E., and Westaway, D. (2000) Copper(II)-induced conformational changes and protease resistance in recombinant and cellular PrP. Effect of protein age and deamidation, *J. Biol. Chem. 275*, 19121−19131.
27. Quaglio, E., Chiesa, R., and Harris, D. A. (2001) Copper converts the cellular prion protein into a protease-resistant species that is distinct from the scrapie isoform, *J. Biol. Chem. 276*, 11432−11438.
28. Nishina, K., Jenks, S., and Supattapone, S. (2004) Ionic strength and transition metals control PrP^{Sc} protease resistance and conversion-inducing activity, *J. Biol. Chem. 279*, 40788−40794.
29. Jones, C. E., Abdelraheim, S. R., Brown, D. R., and Viles, J. H. (2004) Preferential Cu^{2+} coordination by His96 and His111 induces β-sheet formation in the unstructured amyloidogenic region of the prion protein, *J. Biol. Chem. 279*, 32018−32027.
30. Giese, A., Levin, J., Bertsch, U., and Kretzschmar, H. (2004) Effect of metal ions on de novo aggregation of full-length prion protein, *Biochem. Biophys. Res. Commun. 320*, 1240−1246.
31. Bocharova, O. V., Breydo, L., Salnikov, V. V., and Baskakov, I. V. (2005) Copper(II) inhibits in vitro conversion of prion protein into amyloid fibrils, *Biochemistry 44*, 6776−6787.
32. Hijazi, N., Shaked, Y., Rosenmann, H., Ben-Hur, T., and Gabizon, R. (2003) Copper binding to PrPC may inhibit prion disease propagation, *Brain Res. 993*, 192−200.

33. Levin, J., Bertsch, U., Kretzschmar, H., and Giese, A. (2005) Single particle analysis of manganese-induced prion protein aggregates, *Biochem. Biophys. Res. Commun. 329*, 1200−1207.
34. Brown, D. R., Hafiz, F., Glasssmith, L. L., Wong, B. S., Jones, I. M., Clive, C., and Haswell, S. J. (2000) Consequences of manganese replacement of copper for prion protein function and proteinase resistance, *EMBO J. 19*, 1180−1184.
35. Wong, B. S., Brown, D. R., Pan, T., Whiteman, M., Liu, T., Bu, X., Li, R., Gambetti, P., Olesik, J., Rubenstein, R., and Sy, M. S. (2001) Oxidative impairment in scrapie-infected mice is associated with brain metals perturbations and altered antioxidant activities, *J. Neurochem. 79*, 689−698.
36. Bush, A. I. (2003) The metallobiology of Alzheimer's disease, *Trends Neurosci. 26*, 207−214.
37. Ricchelli, F., Drago, D., Filippi, B., Tognon, G., and Zatta, P. (2005) Aluminum-triggered structural modifications and aggregation of β-amyloids, *Cell. Mol. Life Sci. 63*, 1724−1733.
38. McLaurin, J., Yang, D., Yip, C. M., and Fraser, P. E. (2000) Review: modulating factors in amyloid-beta fibril formation, *J. Struct. Biol. 130*, 259−270.
39. Tagliavini, F., Prelli, F., Ghiso, J., Bugiani, O., Serban, D., Prusiner, S. B., Farlow, M. R., Ghetti, B., and Frangione, B. (1991) Amyloid protein of Gerstmann-Straussler-Scheinker disease (Indiana kindred) is an 11 kD fragment of prion protein with an N-terminal glycine at codon 58, *EMBO J. 10*, 513−519.
40. Tagliavini, F., Lievens, P. M., Tranchant, C. Warter, J. M., Mohr, M., Giaccone, G., Perini, F., Rossi, G., Salmona, M., Piccardo, P., Ghetti, B., Beavis, R. C., Bugiani, O., Frangione, B., and Prelli, F. (2001) A 7-kDa prion protein (PrP) fragment, an integral component of the PrP region required for infectivity, is the major amyloid protein in Gerstmann-Straussler-Scheinker disease A117V, *J. Biol. Chem. 276*, 6009−6015.
41. Piccardo, P., Seiler, C., Dlouhy, S. R., Young, K., Farlow, M. R., Prelli, F., Frangione, B., Bugiani, O., Tagliavini, F., and Ghetti, B. (1996) Proteinase-K-resistant prion protein isoforms in Gerstmann-Straussler-Scheinker disease (Indiana kindred), *J. Neuropathol. Exp. Neurol. 55*, 1157−63.
42. Tagliavini, F., Prelli, F., Verga, L., Giaccone, G., Sarma, R., Gorevic, P., Ghetti, B., Passerini, F., Ghibaudi, E., Forloni, G., Samona, G., Bugiani, O., and Frangione, B. (1993) Synthetic peptides homologous to prion protein residues 106−147 form amyloid-like fibrils in vitro, *Proc. Natl. Acad. Sci. U.S.A. 90*, 9678−9682.
43. Tagliavini, F., Forloni, G., Colombo, L., Rossi, G., Girola, L., Canciani, B., Angeretti, N., Giampaolo, L., Peressini, E., Awan, T., De Gioia, L., Ragg, E., Bugiani, O., and Salmona, M. (2000) Tetracycline affects abnormal properties of synthetic PrP peptides and PrP(Sc) in vitro, *J. Mol. Biol. 300*, 1309−1322.
44. Bala Gupta, V., Anitha, S., Hedge, M. L., Zecca, L., Garruto, M. R., Ravid, R., Shankar, S. K., Stein, R., Shanmugavelu, P., and Jagannatha Rao, K. S. (2005) Aluminium in Alzheimer's disease: are we still at a crossroad?, *Cell. Mol. Life Sci. 62*, 143−158.
45. Zatta, P., Zambenedetti, P., Bruna, V., and Filippi, B. (1994) Activation of acetylcholinesterase by aluminum (III): the relevance of the metal species, *NeuroReport 5*, 1777−1780.
46. Uversky, V. N., Li, J., and Fink, A. L. (2001) Metal-triggered structural transformations, aggregation and fibrillation of human alpha-synuclein. A possible molecular link between Parkinson's disease and heavy metal exposure, *J. Biol. Chem. 276*, 44284−44296.
47. LeVine, H. R. (1993) Thioflavine T interaction with synthetic Alzheimer's disease beta-amyloid peptides: detection of amyloid aggregation in solution, *Protein Sci. 2*, 404−410.
48. Thackray, A. M., Knight, R., Haswell, S. J., Bujdoso, R., and Brown, D. R. (2002) Metal imbalance and compromised antioxidant function are early changes in prion disease, *Biochem. J. 362*, 253−258.
49. Checler, F., and Vincent, B. (2002) Alzheimer's and prion diseases: distinct pathologies, common proteolytic denominators, *Trends Neurosci. 25*, 616−620.
50. Kawahara, M. (2005) Effects of aluminum on the nervous system and its possible link with neurodegenerative diseases, *J. Alzheimer's Dis. 8* (2), 171−182.
51. Speziali, M., and Orvini, E. (2003) Metal distribution and regionalization in the brain, in *Metal Ions and Neurodegenerative Disorders* (Zatta, P., ed.), pp 15−65, World Scientific Publishing Co., Mainland Press, Singapore.
52. Hornemann, S., Schorn, C., and Wuthrich, K. (2004) NMR structure of the bovine prion protein isolated from healthy calf brains, *EMBO Rep. 5*, 1159−1164.
53. Ghetti, B., Piccardo, P., Frangine, B., Bugiani, O., Giaccone, G., Young, K., Prelli, F., Farlow, M. R., Dlouhy, S. R., and Tagliavini, F. (1996) Prion protein amyloidosis, *Brain Pathol. 6*, 127−145.
54. Prusiner, S. B. (1991) Molecular biology of prion diseases, *Science 252*, 1515−1522.
55. Muramoto, T., Scott, M., Cohen, F. E., and Prusiner, S. B. (1996) Recombinant scrapie-like prion protein of 106 amino acids is soluble, *Proc. Natl. Acad. Sci. U.S.A. 93*, 15457−15462.
56. Supattapone, S., Bosque, P., Muramoto, T., Wille, H., Aagaard, C., Peretz, D., Nguyen, H. O., Heinrich, C., Torchia, M., Safar, J., Cohen, F. E., DeArmond, S. J., Prusiner, S. B., and Scott, M. (1999) Prion protein of 106 residues creates an artifical transmission barrier for prion replication in transgenic mice, *Cell 96*, 869−878.
57. Salmona, M., Morbin, M., Massignan, T., Colombo, L., Mazzoleni, G., Capobianco, R., Diomede, L., Thaler, F., Mollica, L., Musco, G., Kourie, J. J., Bugiani, O., Sharma, D., Inouye, H., Kirschner, D.A., Forloni, G., and Tagliavini, F. (2003) Structural properties of Gerstmann-Straussler-Scheinker disease amyloid protein, *J. Biol. Chem. 278*, 48146−48153.
58. Sokolowski, F., Modler, A. J., Masuch, R., Zirwer, D., Baier, M., Lutsch, G., Moss, D. A., Gast, K., and Naumann, D. (2003) Formation of critical oligomers is a key event during conformational transition of recombinant Syrian Hamster prion protein, *J. Biol. Chem. 278*, 40481−40492.
59. Tsenkova, R. N., Iordanova, I. K., Toyoda, K., and Brown, D. R. (2004) Prion protein fate governed by metal binding, *Biochem. Biophys. Res. Commun. 325*, 1005−1012.
60. Kim, N. H., Choi, J. K., Jeong, B. H., Kim, J. I., Kwon, M. S., Carp, R. I., and Kim, Y. S. (2005) Effect of transition metals (Mn, Cu, Fe) and deoxycholic acid (DA) on the conversion of PrPC to PrPres, *FASEB J. 19*, 783−785.
61. Garnett, A. P., and Viles, J. H. (2003) Copper binding to the octarepeats of the prion protein. Affinity, specificity, folding, and cooperativity: insights from circular dichroism, *J. Biol. Chem. 278*, 6795−6802.
62. Gaggelli, E., Bernardi, F., Molteni, E., Pogni, R., Valensin, D., Valensin, G., Remelli, M., Luczkowski, M., and Kozlowski, H. (2005) Interaction of the human prion PrP(106−126) sequence with copper(II), manganese(II), and zinc(II): NMR and EPR studies, *J. Am. Chem. Soc. 127*, 996−1006.
63. Fasman, G. D. (1996) Aluminum and Alzheimer's disease: model studies, *Coord. Chem. Rev. 149*, 125−165.
64. Klug, G. M. J. A., Losic, D., Subasinghe, S. S., Aguilar, M.-I, Martin, L. L., and Small, D. H. (2003) β-amyloid protein oligomers induced by metal ions and acid pH are distinct from those generated by slow spontaneous ageing at neutral pH, *Eur. J. Biochem. 270*, 4282−4293.
65. Gu, W., Wang, T., Zhiu, J., Shi, Y, and Liu, H. (2003) Molecular dynamics simulation of the unfolding of the human prion protein domain under low pH and high-temperature conditions, *Biophys. Chem. 104*, 79−49.

BI0601454